Colloids and Surfaces B: Biointerfaces 141 (2016) 528–536

Contents lists available at ScienceDirect

Colloids and Surfaces B: Biointerfaces

journal homepage: www.elsevier.com/locate/colsurfb

Role of amphipathicity and hydrophobicity in the balance between hemolysis and peptide–membrane interactions of three related antimicrobial peptides

Axel Hollmann[a,b,c], Melina Martínez[a], Martín E. Noguera[d], Marcelo T. Augusto[c], Anibal Disalvo[b], Nuno C. Santos[c], Liliana Semorile[a], Paulo C. Maffía[a,*]

[a] Laboratory of Molecular Microbiology, Institute of Basic and Applied Microbiology, National University of Quilmes, Bernal, Buenos Aires, Argentina
[b] Laboratory of Biointerfaces and Biomimetic Systems, CITSE, National University of Santiago del Estero-CONICET, Santiago del Estero, Argentina
[c] Instituto de Medicina Molecular, Faculdade de Medicina, Universidade de Lisboa, Avenida Professor Egas Moniz, 1649-028 Lisbon, Portugal
[d] Instituto de Química y Fisicoquímica Biológicas, CONICET-University of Buenos Aires, Buenos Aires, Argentina

ARTICLE INFO

Article history:
Received 12 October 2015
Received in revised form 30 January 2016
Accepted 2 February 2016
Available online 4 February 2016

Keywords:
CAMPs
Hydrophobicity
Membrane interaction

ABSTRACT

Cationic antimicrobial peptides (CAMPs) represent important self defense molecules in many organisms, including humans. These peptides have a broad spectrum of activities, killing or neutralizing many Gram-negative and Gram-positive bacteria. The emergence of multidrug resistant microbes has stimulated research on the development of alternative antibiotics. In the search for new antibiotics, cationic antimicrobial peptides (CAMPs) offer a viable alternative to conventional antibiotics, as they physically disrupt the bacterial membranes, leading to lysis of microbial membranes and eventually cell death. In particular, the group of linear α-helical cationic peptides has attracted increasing interest from clinical as well as basic research during the last decade.

In this work, we studied the biophysical and microbiological characteristics of three new designed CAMPs. We modified a previously studied CAMP sequence, in order to increase or diminish the hydrophobic face, changing the position of two lysines or replacing three leucines, respectively. These mutations modified the hydrophobic moment of the resulting peptides and allowed us to study the importance of this parameter in the membrane interactions of the peptides. The structural properties of the peptides were also correlated with their membrane-disruptive abilities, antimicrobial activities and hemolysis of human red blood cells.

1. Introduction

Antimicrobial peptides (AMPs) are produced by almost all species of living beings as a component of their innate defense against infections [1–4]. AMPs are typically short peptides with consensus amphiphilic attributes represented by positively charged and hydrophobic amino acids. The mixed cationic and hydrophobic composition of AMPs makes them well suited for interacting with microbial membranes, which typically present anionic surfaces, rich in lipids such as phosphatidylglycerol or cardiolipin oriented toward the outer environment of the bacteria [5]. Cationic AMPs (CAMPs) are very important resources for human therapeutics as lead compounds to counteract the current drug resistance development [6–9].

The lethal step in the mode of action of most CAMPs is the disruption of the microbial plasma membrane. This process is accomplished in two steps: membrane binding, predominantly governed by electrostatic interactions, and membrane insertion/permeation, related to the hydrophobicity of the peptide, which gives the capacity of partitioning into the microbial membrane [5].

The mechanism of action of CAMPs makes them excellent candidates to counteract the actual drug resistance, in part because bacteria needs to make a massive structural change in bacterial cell wall to be resistant to CAMPs. Despite their microbial membrane affinity, amphipathic CAMPs can also interact and disassemble the membrane of eukaryotic cells, particularly erythrocytes. The eukaryotic cell selectivity is a possible undesirable feature of CAMPs, which represent a challenge to be addressed when designing new CAMPs sequences. The difference between a highly antimicrobial or highly hemolytic peptide is the combination of multiple factors, ranging from the primary sequence to the hydrophobicity and the secondary structure [10,11].

* Corresponding author.
E-mail addresses: paulo.maffia@unq.edu.ar, pcmaffia@hotmail.com (P.C. Maffía).

http://dx.doi.org/10.1016/j.colsurfb.2016.02.003
0927-7765/

Model membrane systems, such as lipid vesicles, have been used for three decades to explore the structure, function and mechanism of AMPs [12,13]. Despite the huge contribution from the scientific community in this field, a consensus model of AMP action on model membranes (synthetic layers) is still lacking, probably because of different CAMPs have different modes of membrane action. A way to get an insight on the antimicrobial or hemolytic activity of peptides is to elucidate the mechanism of the AMP-induced bilayer destabilization. In this regard, it is important to identify the AMPs features necessary to display activity, enabling the design of more potent and safer AMPs [14].

In this context, we studied the biophysical and microbiological characteristics of new CAMPs designed from a previously studied CAMP sequence, to gain insights into their structural properties and their membrane-disruptive abilities, antimicrobial activities and hemolysis of human red blood cells.

2. Material and methods

2.1. Peptides synthesis

Each peptide was synthesized with C-terminus amidation. Peptides were synthesized and obtained at a purity grade of >95% by HPLC (GenScript Co., Piscataway, NJ, USA). The peptides sequences were: peptide 5: RIVQRIKKWLLKWKKLGY;

peptide 8: RIVQRILKWLKKWYKLGK; peptide 8.1: RIVQRIAKWAKKWYKAGK.

2.2. Analysis of physicochemical properties

For the analysis of net charge, hydrophobic moment, hydrophobicity, isoelectric point and molecular weight, we used the online programs Heliquest [15] (http://heliquest.ipmc.cnrs.fr/cgi-bin/ComputParamsV2.py), and Agadir (http://agadir.crg.es/) [16]. The mean hydrophobicity (H) and the mean hydrophobic moment (μH) were calculated from the amino acid sequences, using the Eisenberg scale for hydrophobicity by the HydroMCalc applet [10]. The helical wheel projections diagrams were obtained from Heliquest.

2.3. Antimicrobial activity

Minimal inhibitory concentration was determined by standard microdilution assay according to CLSI recommendations [17], using Mueller Hinton Broth (DIFCO) supplemented with Ca^{2+} (20–25 mg/L) and Mg^{2+} (10–12.5 mg/L). The bacterial strains used were *Pseudomonas aeruginosa* ATCC® 47085 and *Staphylococcus aureus* ATCC® 25923.

2.4. Hemolytic assay

The hemolytic activity of the peptides was evaluated according to the method described previously [18]. Briefly, a volume of heparinized human whole blood was diluted 3× in phosphate-buffered saline and then centrifuged at 1500 rpm for 10 min. This procedure was repeated three more times. The cellular pellet was resuspended in phosphate-buffered saline to a final dilution of 0.5% (*v*/*v*). Peptides were then added at different concentrations and incubated at 37 °C for 30 min. Afterwards, tubes were centrifuged and the absorbance of the supernatant at 550 nm was measured. The percentage lysis was then calculated relative to 0% lysis with buffer and 100% lysis with water. The absorbance measurement was repeated three times, and the averaged values were used.

2.5. Circular dichroism in the far UV

We studied the secondary structure content by circular dichroism (CD) spectroscopy in the far UV, using a JASCO J-810 (Jasco Corp., Tokyo, Japan) spectropolarimeter, calibrated with (+)-10-camphorsulfonic acid. The measurements were performed under nitrogen gas flow of 8 L/h at a temperature of 20 °C, controlled by a Peltier system (JASCO).

Spectra were recorded between 185 and 320 nm, using a 0.1 cm path-length cell. The peptide concentrations were 20 μM, dissolved in 10 mM sodium phosphate buffer pH 7.0, or the same buffer with sodium 10 mM dodecyl sulphate (SDS). The sensitivity was 100 millidegrees. We used a scan speed of 50 nm/min, a response time of 1 s and a bandwidth of 1 nm. We performed an average of five assays for each sample spectra. The average absorption was corrected by buffer and then baselined to zero using the average of readings between 290 and 320 nm. Finally, the data were smoothed using a Savizky–Golay fourth-degree polynomial, with a window of ten points. The spectra were converted to mean molar ellipticity per residue using the relationship:

$$[\theta] = \frac{\theta}{10 \times c \times n \times d} \quad (1)$$

where $[\theta]$ is the molar ellipticity (in degrees × cm^2 × $dmol^{-1}$), θ the ellipticity in millidegrees, n is the number of residues of the peptide and c its molar concentration, d is the length of the cell in centimeters.

The %AH (or α-helical content) was calculated by following equation described in Ref. [19].

$$\%AH = \frac{(\theta_{222} + 2000) \times 100}{-30000} \quad (2)$$

2.6. Lipids

The zwitterionc lipid DMPC (1,2-dimyristoyl-sn-glycero-3-phosphocholine) and negatively charged lipid DMPG (1,2-dimyristoyl-sn-glycero-3-phospho-1′-rac-glycerol) were purchased from Avanti Polar Lipids (Alabaster, AL, USA). 5NS (5-DOXYL-stearic acid) and 16NS (16-DOXIL-stearic acid) were also purchased from Sigma.

The working buffer was HEPES 10 mM pH 7.4 in NaCl 150 mM.

2.7. Fluorescence spectroscopy measurements

Since peptides 5, 8 and 8.1 contain 2 tryptophan residues each, fluorescence techniques are suitable tools for the analyses of these molecules. Membrane partition and fluorescence quenching studies were carried out in a Varian Cary Eclipse fluorescence spectrophotometer (Mulgrave, Australia). The fluorescence spectral characterization of peptides and Trp was performed at 280 nm excitation wavelength, except for the quenching experiments that was performed at 290 nm to minimize the relative quencher/fluorophore light-absorption ratios. For the quenching experiments, fluorescence emission was collected at 350 nm (fixed wavelength). For the partition studies, integrated spectra from 310 to 450 nm were used. Typical spectral bandwidths were 5 nm for excitation and 10 nm for emission. Excitation and emission spectra were corrected for wavelength-dependent instrumental factors [20,21]. During the quenching and partition experiments, emission was also corrected for successive dilutions, scatter [21] and simultaneous light absorptions of quencher and fluorophore.

2.8. Partition coefficient determination

Large unilamellar vesicles (LUV) were prepared by extrusion methods, as described elsewhere [22,23].

Membrane partition studies were performed by successive additions of small amounts of different lipid systems to a 5 μM peptide solution, with 10 min incubation at 25 °C. Lipid systems included DMPC and DMPC:POPG (5:1) in order to mimic bacterial membrane [24]. The partition coefficients (K_p) were calculated fitting the experimental data into Eq. (3) [25]:

$$\frac{I}{I_W} = \frac{1 + K_p \gamma_L \frac{I_L}{I_W} [L]}{1 + K_p \gamma_L [L]} \quad (3)$$

where I_W and I_L are the fluorescence intensities in aqueous solution and in lipid, respectively, γ_L is the molar volume of the lipid [26] and [L] its concentration.

2.9. Surface pressure

Changes on the surface pressure of lipid monolayers induced by peptides 5, 8 and 8.1 were measured in a Kibron Langmuir–Blodgett trough, at constant temperature (25 ± 0.5 °C). The surface of the buffer solution contained in a Teflon trough of fixed area was exhaustively cleaned by surface aspiration. Then, a chloroform solution of lipids was spread on this surface to reach surface pressures of 20.5 ± 1 mN/m. Peptide solutions were injected in the subphase and the changes of surface pressure were recorded until a constant value was reached.

Pressure data obtained were fitted with the follow equation:

$$\theta = \frac{\Delta\Pi}{\Delta\Pi_{max}} = \frac{[\text{peptide}]^n}{K_d + [\text{peptide}]^n} \quad (4)$$

where θ corresponds to the degree of coverage, ΔP is the surface pressure shift, [peptide] is the peptide concentration, n is the heterogeneity parameter describing the width of energy distribution and K_d is the dissociation constant.

2.10. Acrylamide quenching

The fluorescence quenching of peptides (5 μM) by acrylamide was measured in buffer and in the presence of DMPC:DMPG (5:1) LUV (3 mM), by successive additions of small volumes of the quencher stock solution, ranging from 0 to 60 mM [27]. Each spectrum was recorded after 10 min incubation. Quenching data were analyzed using the Stern–Volmer equation [28]:

$$\frac{I_0}{I} = 1 + K_{SV} \times [Q] \quad (5)$$

where I and I_0 are the fluorescence intensities of the sample in the presence and absence of quencher respectively, K_{SV} is the Stern–Volmer constant and [Q] is the quencher concentration.

2.11. 5NS and 16NS quenching

Fluorescence quenching assays with the lipophilic probes 5NS and 16NS were carried out at the same peptide and lipid concentrations used for the acrylamide quenching study. Briefly, by successive additions of small amounts of these quenchers in ethanol solution to the peptide samples in DMPC:DMPG (5:1), keeping the ethanol concentration below 2% (v/v) [29]. The effective lipophilic quencher concentration in the membrane was calculated from the partition coefficient of both quenchers to the lipid bilayers [30]. After each quencher addition, samples were incubated for 10 min before measurement. Quenching data were analyzed by using the Stern–Volmer equation (Eq. (5)), or the Lehrer equation (Eq. (6)) when a negative deviation from the Stern–Volmer relationship is observed [30,31].

$$\frac{I_0}{I} = \frac{1 + K_{SV}[Q]}{(1 + K_{SV}[Q])(1 - f_b) + f_b} \quad (6)$$

where f_b corresponds to the fraction of light arising from the fluorophores accessible to the quencher.

2.12 Membrane dipole potential assessed by di-8-ANEPPS

Human blood samples were obtained from healthy volunteers, with their previous written informed consent, at the Instituto Português do Sangue (Lisbon, Portugal). This study was approved by the ethics committee of the Faculdade de Medicina da Universidade de Lisboa. Isolation of erythrocytes and labeling of these cells with di-8-ANEPPS (Invitrogen, Carlsbad, CA, USA) were performed as described before [32,33]. For erythrocytes isolation, blood samples were centrifuged at 1200 × g during 10 min, plasma and buffy-coat were removed, and remaining erythrocytes were washed twice in working buffer. They were incubated at 1% hematocrit in buffer supplemented with 0.05% (m/v) Pluronic F-127 (Sigma) and di-8-ANEPPS 10 μM. Cells were incubated with the fluorescent probe during 1 h, with gentle agitation, and unbound probe was washed with Pluronic-free buffer on two centrifugation cycles. Peptide 5, peptide 8 and peptide 8.1 were incubated with erythrocytes at 0.02% hematocrit during 1 h, with gentle agitation, before the fluorescence measurements. Excitation spectra and the ratio of intensities at the excitation wavelengths of 455 and 525 nm ($R = I_{455}/I_{525}$) were obtained with emission set at 670 nm to avoid membrane fluidity-related artifacts. [34,35]. Excitation and emission slits for these measurements were set to 5 and 10 nm, respectively. The variation of R with the peptide concentration was analyzed by a single binding site model [36]:

$$\frac{R}{R_0} = 1 + \frac{\frac{R_{min}}{R_0}[\text{peptide}]}{K_d + [\text{peptide}]} \quad (7)$$

with the R values normalized for R_0, the value in the absence of peptide. R_{min} defines the asymptotic minimum value of R and K_d is the dissociation constant.

3. Results

3.1. Peptide design

In a previous work, we had designed and synthesized a group of new CAMPs, and tested them against a panel of 82 clinical isolates expressing different mechanisms of drug resistance. From that group, peptide 5 exhibited antimicrobial activity comparable to, or even better than the comparator Omiganan (MBI-226). This CAMP also showed higher activity against some Gram positive bacteria from the genus *Staphylococcus* [37]. For this study, we designed and analyzed two mutated versions of peptide 5 (peptide 8 and peptide 8.1), with the objective of gaining further insights into their biophysical interactions with biological membranes and the role of the hydrophobic moment as a modulator of antibacterial and haemolytic activity. Peptide 8 was obtained by exchanging two lysines (K7 and K14) located adjacent in the alpha helical wheel projection, which were disrupting the hydrophobic face of peptide 5 (Fig. 1A). These two lysines were exchanged for the two adjacent hydrophobic amino acids in the α-helical wheel projection, tyrosine (Y18) and leucine (L11) (Fig. 1A). This rearrangement of two pairs of amino acids creates an undisrupted hydrophobic face when the peptide structures as an alpha helix.

Peptide 8.1 was obtained from peptide 8 replacing three leucines (L7, L10 and L16) for three alanines, a small midrange hydrophobic amino acid with frequent occurrence in membrane domains. This replacement was hypothesized to diminish the hydrophobic moment and hence to decrease its possible hemolytic activity.

When analyzing the physicochemical parameters of the three peptides we could see that, as expected, the isoelectric point and the net charge remains unchanged in the three sequences (Table 1). Peptide 8 and 8.1, they both have an increased

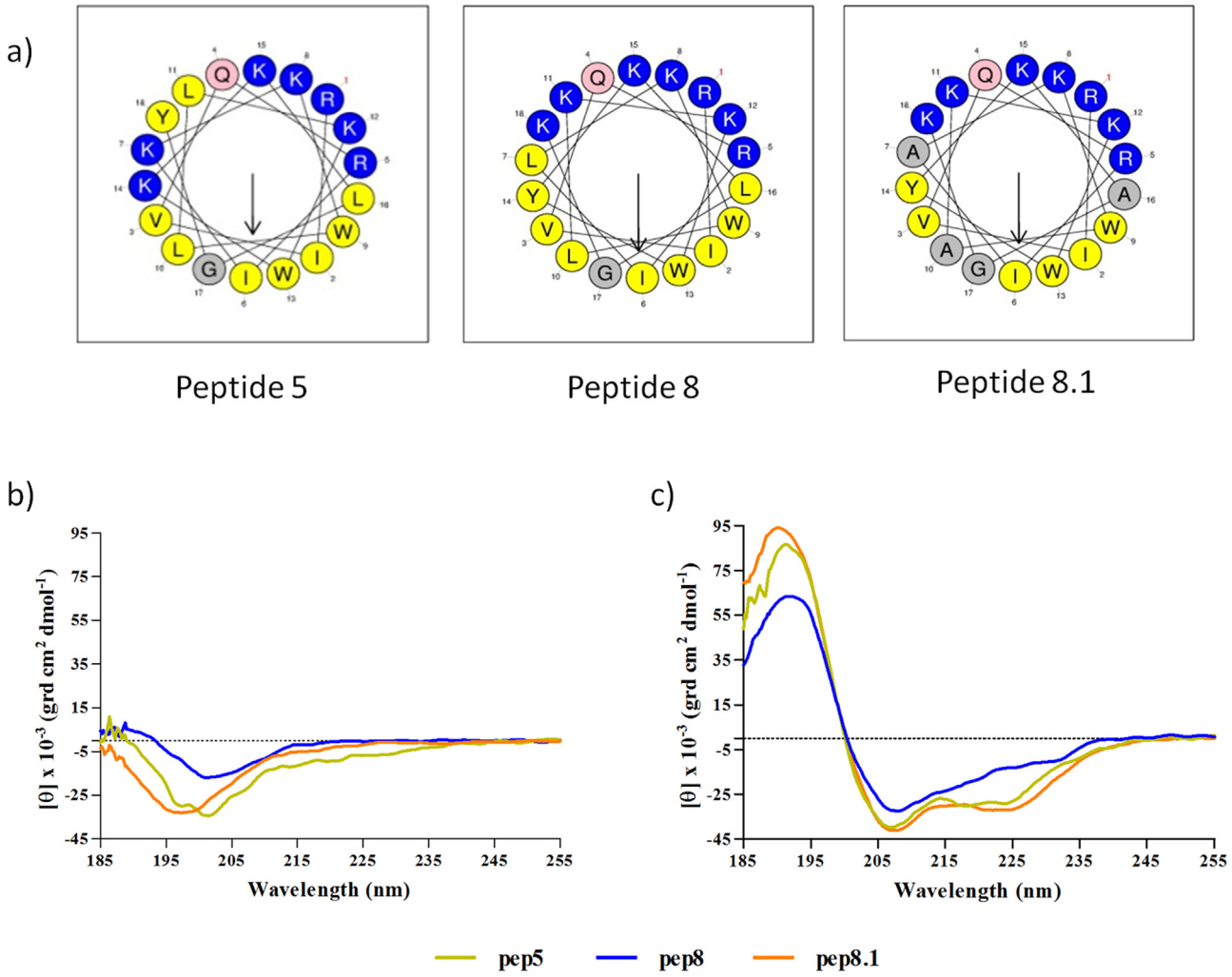

Fig. 1. (a) Helical wheel projection of the peptides. Peptide 8 was obtained from peptide 5, after exchanging K7 and K14 for Y18 and L11. This change rendered two well defined faces, one hydrophobic and the other hydrophilic. Peptide 8.1 was obtained when the three L from peptide 8 where replaced for A. Graphics were obtained from HeliQuest. Yellow circles represent hydrophobic residues and blue circles the positively-charged aminoacids. The arrow depicts the hydrophobic moment. (b) and (c) CD spectra of CAMPs in aqueous solution and SDS micelles. The spectra were measured at 20 μM each CAMP, in 10 mM sodium phosphate pH 7.0 in the absence (panel b) or presence (panel c) of 10 mM SDS. (For interpretation of the references to color in this figure legend, the reader is referred to the web version of this article.)

Table 1
Physicochemical parameters and biological activity of the three peptides. MW: molecular weigth (daltons), pI: isoelectric point, NC: net charge, μH: hydrophobic moment, H: hydrophobicity, %AH: α-helix content. The α-helix percentege were determined based on circular dichroism spectra calculated as the mean residue molar ellipticity at 222 nm, in SDS micelles. MW in Dalton, pI, NC, μH and H were calculated *in silico* in *http://web.expasy.org/compute_pi/, **http://heliquest.ipmc.cnrs.fr/cgi-bin/ComputParamsV2.py. Minimum inhibitory concentrations (MIC) were determined as the lowest concentration of the peptides that inhibited bacteria growth. P.a. *Pseudomonas aeruginosa*, S.a. *Staphylococcus aureus*.The tests were performed at least three times in triplicate. Hemolytic activity is shown as a percentage (%) of hemolysis compared to distilled water (100% hemolysis) ± standard deviation (SD), $n = 3$.

Peptide	Physicochemical parameters						MIC (μM)		%Hemolysis
	MW*	pI*	NC**	μH**	H**	%AH	P.a	S.a	55 μM
Pep 5	2356.98	11.26	7	0.58	0.455	88	54	3.4	8 ± 2
Pep 8	2356.98	11.26	7	0.741	0.455	42	27	13.6	85 ± 12
Pep 8.1	2330.73	11.26	7	0.681	0.223	100	55	13.7	5 ± 1

hydrophobic moment compared to the parent peptide 5. Nevertheless, in terms of hydrophobicity, the positional exchange of two lysines for a tyrosine and a leucine did not produce any change in peptide 8, but the replacement of three leucines for three alanines decreased the hydrophobicity in peptide 8.1 (Table 1).

3.2. Antimicrobial and hemolytic activity

The activity of the three peptides was analyzed comparing the antimicrobial and hemolytic activities (Table 1). The antimicrobial activity was studied in two different types of bacteria, *P. aeruginosa* (Gram negative) and *S. aureus* (Gram positive). The hemolytic activity has dramatically increased from peptide 5 to peptide 8. On the other hand, replacing three Leu for Ala, restored (or even improved) the low hemolytic capacity of peptide 8.1, but led to the original higher MIC against *P. aeruginosa* and decreased the activity against *S. aureus*.

This substitution (from peptide 8 to peptide 8.1) also restored the MIC values for *P. aeruginosa*, but impaired the antimicrobial activity for *S. aureus*. It is probable that the three Leu are important for the peptide to interact with Gram negative bacterial membranes.

In order to rationalize the results obtained in bacteria, we decided to conduct a biophysical characterization of the peptides and its interaction with model and erythrocyte membranes.

3.3. Helical induction of CAMPs in SDS micelles

The circular dichroism spectra of peptides in aqueous solution showed that they are all unstructured in aqueous buffer, with a characteristic minimum at approximately 200 nm (Fig. 1B). With the addition of SDS micelles (Fig. 1C), conformational changes occurred in the three peptides, which are consistent with the formation of α-helix structure with two characteristic minima near 208 and 222 nm.

When comparing the percentage of α-helix of the three peptides, it can be seen that the redistribution of the two pairs of amino acids in peptide 8 produced a significant decrease in the alpha helix content. In contrast, the replacing of three leucines for alanines in peptide 8.1, induced an increase of the percentage of α-helix content in the peptide (Fig. 1C, and Table 1).

3.4. Membrane partition studies by Trp fluorescence

UV-visible absorption and fluorescence spectra in buffer of peptides are comparable to those of Trp, besides a small red shift on emission spectra found for peptide 5, indicating some changes in the Trp surrounding environment of this peptide in aqueous solution (Fig. 2A). As shown in Fig. 2C, the Trp fluorescence intensity of the peptides 5 and 8 increases in the presence of LUV made of DMPC, a zwiterionc lipid. The partition coefficient between the lipid and aqueous phases, K_p, determined by fitting the fluorescence intensity data in Eq. (3), are presented in Table 2.

Interestingly, in the case of peptide 8.1, no significant changes in the fluorescence intensity were observed in the presence of DMPC membranes, indicating that this peptide is not able to significantly interact with these neutral lipid membranes, or at least the Trp residues of the peptide are not involved in the interaction, considering that this experiment follows the changes on the Trp environment. When anionic membranes were tested by the addition of DMPG, all peptides presented a higher K_p, meaning a higher affinity for these membranes. This is a relevant result because PG is the second major phospholipid component of bacterial plasma membranes [38].

These results reveal that PG is relevant to enhance the interaction of peptides, but partition is also feasible in neutral lipids for peptide 5 and 8.

3.5. Surface pressure perturbation of monolayers

The interaction of peptides with lipid surfaces was also studied by their effect on the monolayers surface pressure ($\Delta\Pi$), produced by peptides injected in the subphase underneath lipid monolayers stabilized on the air–water interface. As revealed in Fig. 3, $\Delta\Pi$ values resulting from the peptide interaction with DMPC or DMPC:DMPG monolayers at the air–water interface change with the increasing concentration of peptide in the surface. In agreement with partition data, peptide 8 is able to induce the highest changes on the lipid monolayer, followed by peptide 5. Beside Trp partition results showed no interaction between peptide 8.1 and pure DMPC membranes, surface pressure results indicated that this peptide is also able to induce changes on the surface pressure. However, $\Delta\Pi$ values obtained with peptide 8.1 are less than a half of those obtained with peptides 5 and 8, confirming a weak interaction of this peptide with zwitterionic DMPC membranes. In contrast, in DMPC:DMPG monolayers the behavior of the three peptides are much more homogeneous, although peptide 8 still exhibits the highest affinity values (Table 2).

3.6. Localization of the peptides in the lipid bilayer

In order to test the accessibility of the fluorophores (Trp in these peptides) to the aqueous environment, the fluorescence quenching by acrylamide of the Trp residues of three peptides was studied. Acrylamide is an aqueous soluble quencher that presents a low capacity of penetration into lipid bilayers. If the Trp residue inserts in the membrane, it will be less accessible or inaccessible to the quencher in aqueous solution and, therefore, its fluorescence will be less quenched or not quenched at all [39,40].

Linear Stern–Volmer plots were obtained both in the presence and absence of lipids (DMPC:DMPG) (Fig. 4). The three peptides yielded lower K_{sv} values in the presence of lipids than in their absence, confirming a lipid interaction of the peptides. Also, the linear plots of fluorescence quenching revealed that no hydrophobic pockets were present. Although the existence of hydrophobic pockets does not seem likely in a small peptide, aggregation or clustering could eventually take place.

5 and 16 NS were used to evaluate the in-depth location of the Trp residues of the peptides inserted in DMPC:DMPG vesicles. 5NS is a better quencher for molecules inserted in the membrane in a shallow position, close to the lipid–water interface, while 16NS quenches better molecules buried deeply in the membrane [41]. Stern–Volmer plots are shown in Fig. 4B and C. Fluorescence quenching data enabled the application of the SIMEXDA method [41] to obtain the in-depth distribution of the Trp residues (Fig. 4D). The calculated distance from the center of the bilayer indicates that three peptides are located close to the membrane–water interface, with Trp inserted near the polar head-acyl chain interface. Peptide 8 seems to be located slightly deeper in the membrane (11.2 Å) and peptide 8.1 in a shallower position (12.8 Å) in comparison with original peptide 5 (12.2 Å).

3.7. Interaction of the peptides with red blood cell membranes

Finally, after the characterization of the peptides interaction with the membrane model systems, we studied the peptide–membrane interaction with red blood cells, in order to complement the hemolytic data. We used isolated human erythrocytes labeled with the fluorescent probe di-8-ANEPPS because in previous studies it proved to be a good reporter for the interaction of peptides with the plasma membranes of these cells [42,43].

The membrane dipole potential significantly decreased in the presence of peptide 8, in contrast to peptides 5 and 8.1 where the effect was almost insignificant (Fig. 5). These results are in good agreement with the hemolytic data listed in Table 1 where peptide 8 shows 85% of hemolysis at 55 μM. We can also conclude that at least in this set of peptides the main factor that drives the hemolysis is related with the affinity of the peptides toward the erythrocyte membrane.

4. Discussion

Amphipathicity is hypothesized to be a requirement for CAMPs activity when they are structured as α-helix, however, perfect amphipathicity possibly results in a simultaneous increase in the bactericidal activity and hemolysis [10]. In this regard, it has been previously reported that the interaction between the hydrophobicity levels and the differential distribution of positive residues along the sequence of a CAMP, is a main determinant of bioactivity [11].

It is also accepted that peptides with higher hydrophobicity can readily enter zwitterionic membranes and cause hemolytic effects [44]. In this context, we decided to correlate the affinity membrane

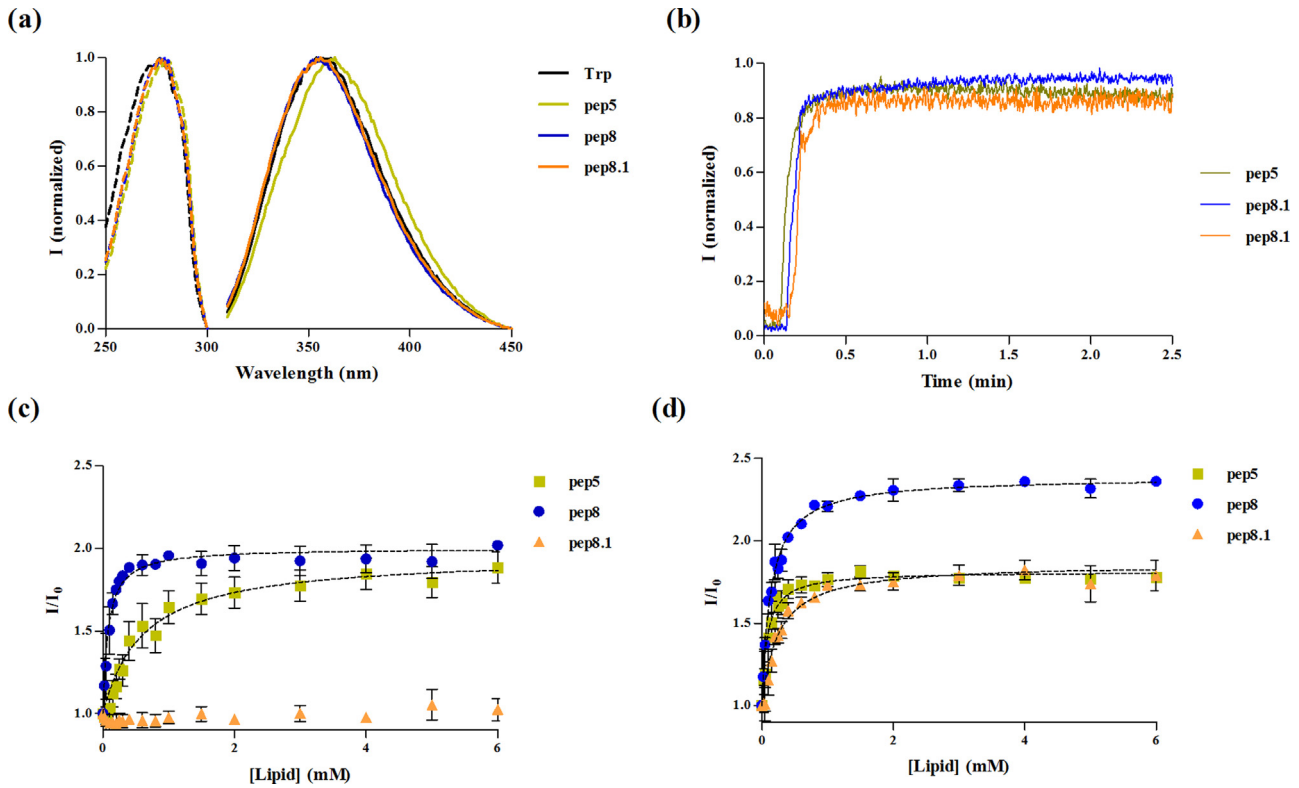

Fig. 2. Normalized fluorescence excitation (dashed line) and emission (solid line) spectra for Trp and peptide 5, peptide 8 and peptide 8.1 (5 μM) (a). Variation of the Trp fluorescence intensity as function of time after addition of LUVs composed of DMPC (b). Partition study of the peptides into lipid vesicles. Variation of the Trp fluorescence intensity as function of addition of LUV composed by pure DMPC (c) or DMPC:DMPG (5:1) (d). Values on panels C and D are presented as mean ± standard deviation (SD); $n = 3$.

Table 2
Partition coefficients (Kp) and I_L/I_W obtained from the fitting of the fluorescence data of the partition assays to Eq. (3). Dissociation constants, K_d, and $\Delta\Pi_{max}$ determined from surface pressure changes obtaining from the fitting of the surface pressure data using Eq. (4). All measures were made at least in triplicate. Values are presented as mean ± standard deviation (SD).

Peptide	Lipid composition	$K_p \times 10^3$	I_L/I_W	K_d	$\Delta\Pi_{max}$
Pep 5	DMPC	2.15 ± 0.41	1.95 ± 0.05	1.06 ± 0.20	11.95 ± 0.83
	DMPC:DMPG (5:1)	16.28 ± 1.69	1.82 ± 0.02	0.30 ± 0.07	11.90 ± 0.50
Pep 8	DMPC	37.68 ± 11.14	2.00 ± 0.01	0.40 ± 0.15	13.65 ± 0.93
	DMPC:DMPG (5:1)	9.69 ± 0.74	2.37 ± 0.02	0.18 ± 0.07	13.64 ± 0.65
Pep 8.1	DMPC	–	–	0.71 ± 0.22	6.91 ± 0.63
	DMPC:DMPG (5:1)	5.23 ± 0.64	1.86 ± 0.02	0.15 ± 0.13	12.17 ± 1.11

of our peptides, each one with a different hydrophobic moment, with their respective antimicrobial and hemolytic activity, in an attempt to correlate this parameter with their biological activity. As was previously pointed, the parent peptide 5 was modified to obtain peptide 8, in which two lysines were exchanged for the two adjacent amino acids: tyrosine (Y18) and leucine (L11), resulting in a sequence with the same hydrophobicity, net charge, and slightly diminished helicity, but with extremely increased hemolytic levels (Table 1). This amino acid positional exchange produced an extreme modification in the red blood cell membrane affinity, as seen in the differential spectra of di-8-ANEPPS bound to erythrocytes. The switch to a highly amphipatic α-helical structure and therefore with a higher hydrophobic moment could be responsible for this dramatic change in the red blood cell membrane affinity of the peptide, explaining its increased hemolytic activity.

Recently, it has been shown that disrupting perfect amphipathicity of α-helical structure can maintain strong antimicrobial activity, reduce hemolytic activity and promote pore formation [45]. For peptide 8.1, a decrease in activity toward *S. aureus, P. aeruginosa* and erythrocytes (in comparison with peptide 8) was directly related to decreasing the hydrophobicity of the hydrophobic face and red blood cell membrane affinity. Therefore, the substitution of Leu residues with Ala residues led to an overall decreased activity, but the hemolytic effect (affinity for eukariotic membranes) was dramatically diminished. In this case, the shift could be due to the diminished hydrophobicity of peptide 8.1 as a result of these replacements.

It is usually accepted that the understanding of the interaction between AMPs and membranes (using lipid membrane models and cells) represents a key aspect to elucidate their mechanism of action [12,46]. It is well known that the membranotropic behavior of a peptide can increase its local concentration at the membrane level, boosting the efficiency of a drug [47]. Here we showed by surface pressure and fluorescent partition data that three peptides exhibit higher affinity toward negatively charged membranes, as expected due its net positive charge. However, the fact that the peptides also interact with zwitterionic membranes (specially for peptides 5 and 8) means that hydrophobic contacts may also play an important role in addition to electrostatic interactions, driving the peptide to its insertion into the lipid monolayers.

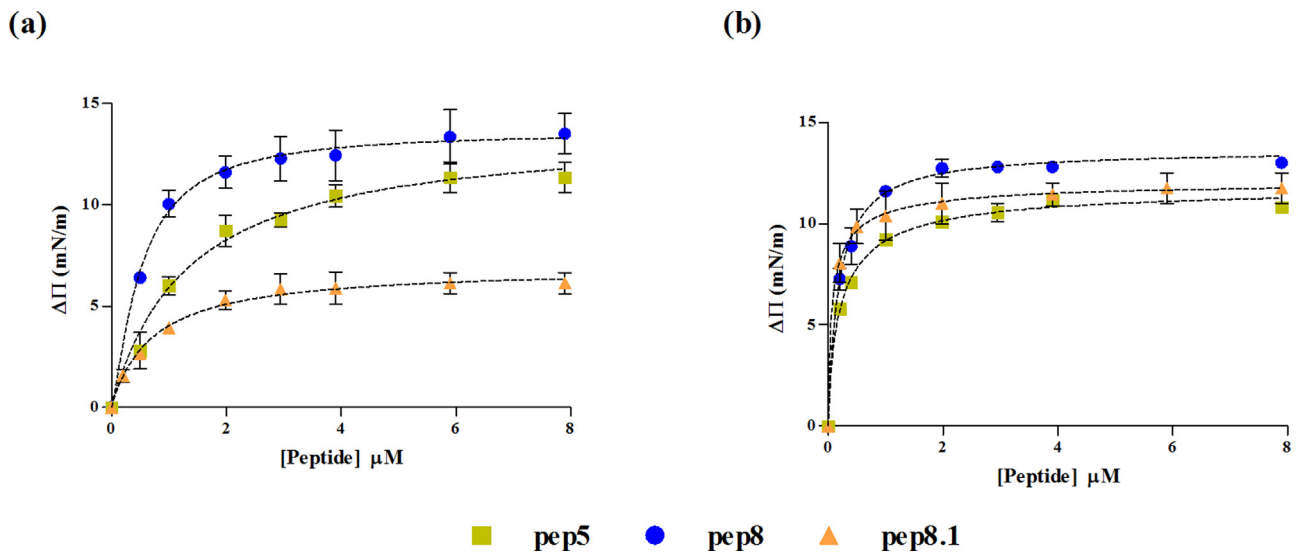

Fig. 3. Interaction of peptides with lipid monolayers. Changes in the surface pressure expressed as $\Delta\Pi$ as a function of the peptide concentration on pure DMPC monolayers (a) or DMPC:DMPG (5:1) monolayers (b). The initial pressure was 21 ± 1 mN/m for all assays. Values are presented as mean ± standard deviation (SD); $n = 3$.

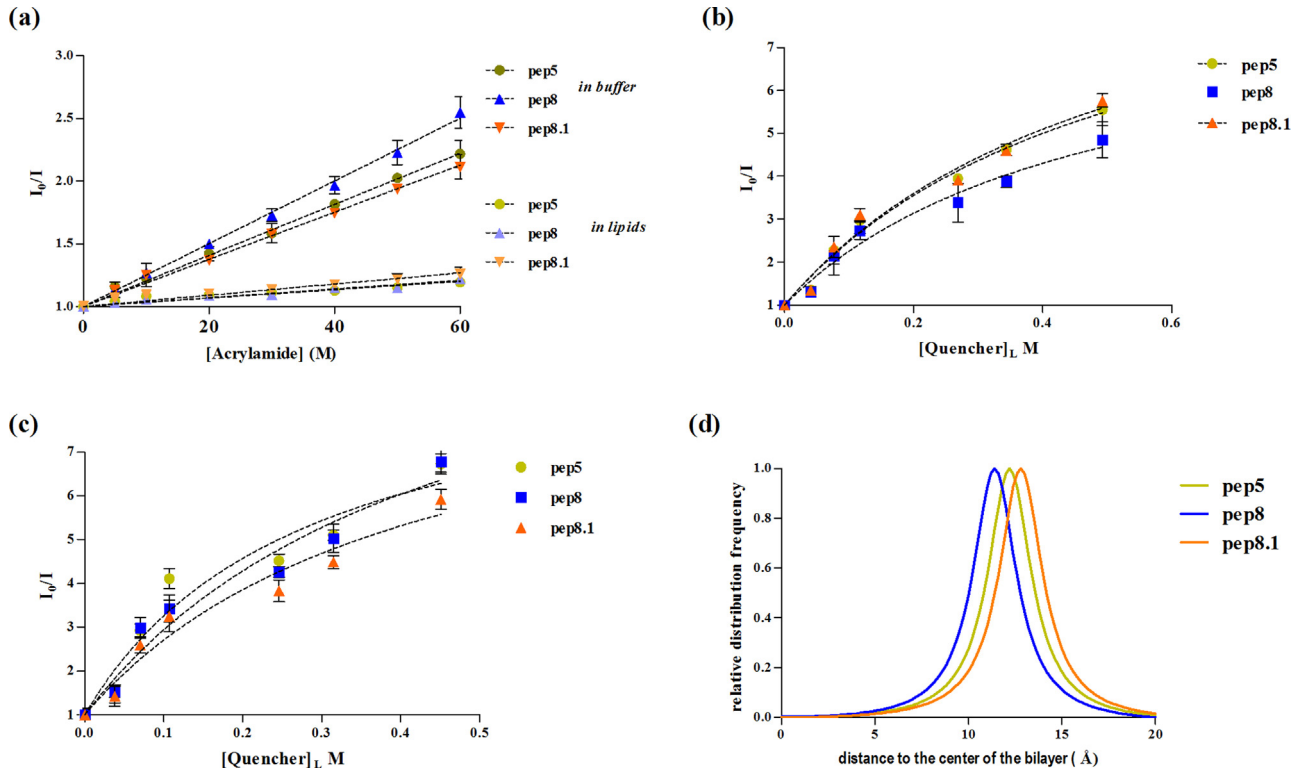

Fig. 4. Localization of the peptides in the bilayer. Fluorescence quenching of 10 μM peptides by acrylamide in the presence and absence of lipid vesicles (a). Fluorescence quenching of peptides by 5NS (b) and 16NS (c) in the bilayer composed by DMPC:DMPG (5:1) 3 mM. In-depth localization (d) of both peptides Trp residues of three peptides inside the membrane using the SIMEXDA method. Values on panels A, B and C are presented as mean ± standard deviation (SD); $n = 3$.

It is also worthy to notice that the linear plots of fluorescence quenching seems to reveal that no hydrophobic pockets were present. It has been previously reported that high core segmental hydrophobicity can lead to an increased potential to peptide self-association at the membrane surface, and also that increases in hydrophobicity will cause stronger peptide dimerization in solution [44], but in these peptides aggregation could probably be prevented by the positively charged residues of the peptides. When the position of Trp residues into the membrane was studied, we found that Trp residues were buried around 8 Å into the membrane. Although Fig. 4D represents the average position of both Trp for each peptide, the half-width at half-height distributions found for the three peptides was narrow (1.44 Å). These results could easily be explained considering that both Trp residues of each peptide accommodate at the membrane surface in a similar position, buried around 8 Å into the bilayer, indicating a membrane parallel position (Fig. 6), in good agreement with other CAMPs [48,49]. According to our results, primarily our peptides should reach the membrane through a process governed by electrostatic forces. Afterwards, a conversion of the peptide into amphipathic α-helical structure

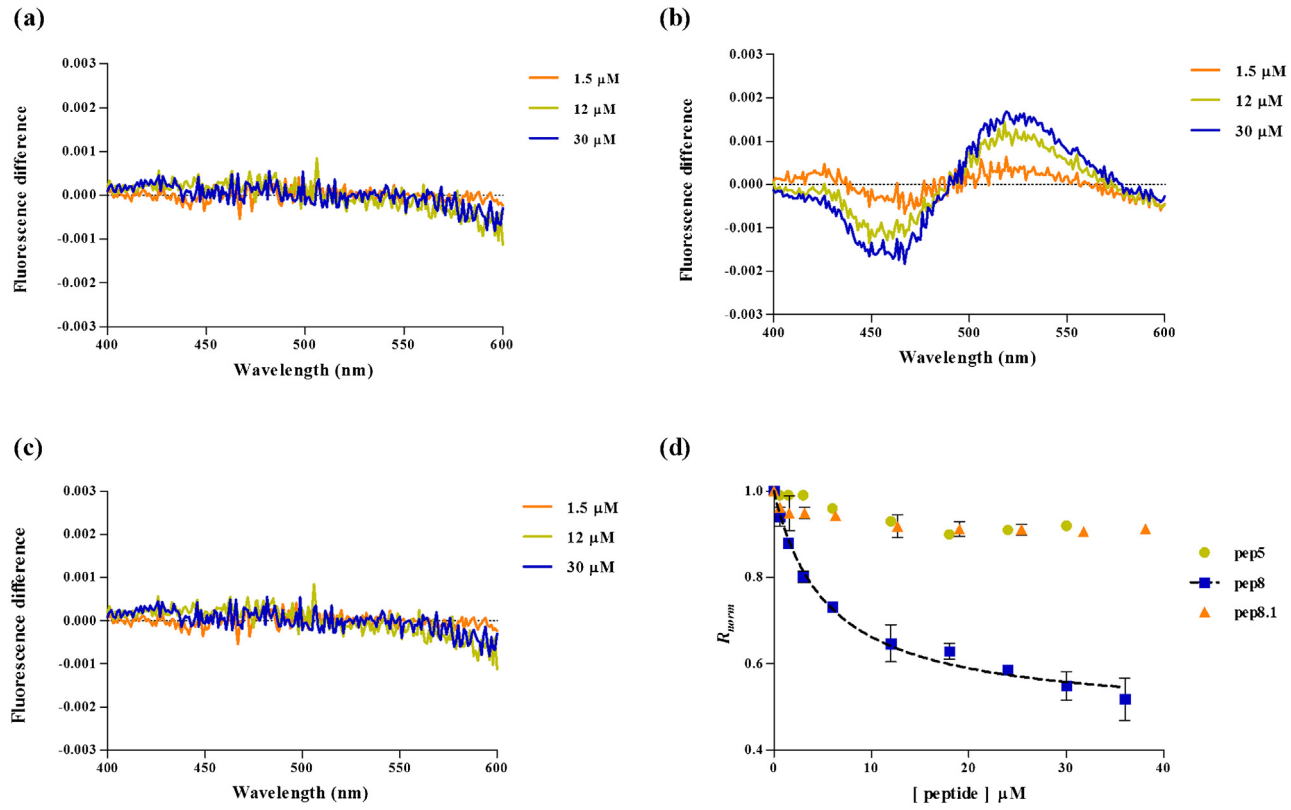

Fig. 5. Antimicrobial peptides interactions with red blood cells. Differential spectra of di-8-ANEPPS bound to erythrocytes membranes in the presence of different concentrations of peptides 5 (a), 8 (b) and 8.1 (c). Spectra were obtained by subtracting the excitation spectrum (normalized to the integrated areas) of labeled cells in the presence of the peptide from the spectrum in the absence of the respective peptide. The shift to the red (decrease in dipole potential) is peptide concentration-dependent. Binding profiles of peptides to erythrocytes cell membranes by plotting the di-8-ANEPPS excitation ratio, R (I_{455}/I_{525}, normalized to the initial value), as a function of the peptide concentration (D). Values on panel D are presented as mean ± standard deviation (SD); $n = 3$.

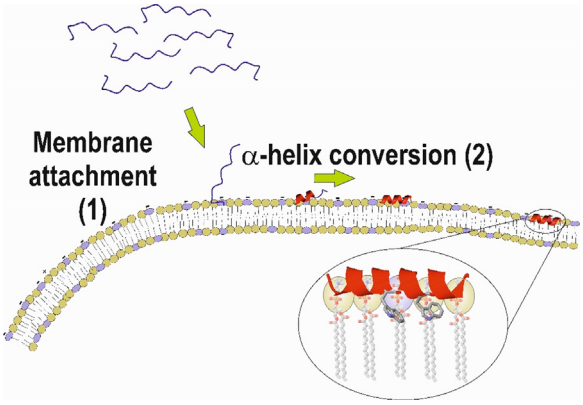

Fig. 6. Scheme of the first steps on putative mode of action of the AMPs presented in this work. It was demonstrated that peptides interact with negatively charged membranes (1), with a concomitant structural conversion from random coil to α-helix (2). Afterwards, the peptides concentrate in a parallel alignment with the membrane, promoting changes in the lipid organization. We hypothetisized that these peptides disposition could trigger the membrane destabilization and lead the antimicrobial activity.

takes place, as showed in our CD data. This conformational changes result in the alignment of the Trp on the same face of the α-helix structured peptide. Finally, the insertion of the Trp residues in the carbon-chain region of the membrane, stabilized by a parallel alignment with the membrane, promotes changes in the lipids organization that triggers the antimicrobial activity (Fig. 6), as was previously reported for CAMPs that follow a carpet-like mechanism [50–52]. In this model, we propose that peptide insertion near the lipid–water interface results in the expansion of the outer leaflet of the bilayer, with accumulation of bound peptide, leading to membrane thinning as a prelude to detergent-like disintegration of the bilayer [53,54], but further experiments should be done to fully prove it. Even though the three peptides seem to follow the same antimicrobial pathway, as pointed above, other factors should be evaluated in order to a rational design of novel CAMPs, specially related to the cytotoxic undesirable effects.

Conflicts of interest

The authors declare no financial or commercial conflict of interest.

Acknowledgements

This work was supported by grants from Universidad Nacional de Quilmes, Comisión de Investigaciones Científicas de la Provincia de Buenos Aires (CIC-BA) and Agencia Nacional de Promoción Científica y Tecnologica (ANPCyT-MINCyT), Argentina; PICT 2013-1481 and PICT 2013-815. The work was also supported by Fundação para a Ciência e a Tecnologia – Ministério da Ciência, Tecnologia e Ensino Superior (FCT-MCTES, Portugal). LS is member of the Research Career of CIC.BA. AH, EAD and PM are members of the Carrera del Investigador Científico y Tecnológico (CONICET, Argentina). MM and MEN acknowledge fellowships from CONICET and MTA has a fellowship SFRH/BD/95624/2013 from Fundação para a Ciência e Tecnologia–Ministério da Educação e Ciência (FCT-MEC, Portugal).

Appendix A. Supplementary data

Supplementary data associated with this article can be found, in the online version, at http://dx.doi.org/10.1016/j.colsurfb.2016.02.003.

References

[1] A. Menendez, R.B. Ferreira, B.B. Finlay, Defensins keep the peace too, Nat. Immunol. 11 (2010) 49–50.
[2] R.E. Hancock, G. Diamond, The role of cationic antimicrobial peptides in innate host defences, Trends Microbiol. 8 (2000) 402–410.
[3] T. Ganz, Defensins: antimicrobial peptides of innate immunity, Nat. Rev. Immunol. 3 (2003) 710–720.
[4] B. Rivas-Santiago, C.J. Serrano, J.A. Enciso-Moreno, Susceptibility to infectious diseases based on antimicrobial peptide production, Infect. Immun. 77 (2009) 4690–4695.
[5] N. Papo, Y. Shai, Can we predict biological activity of antimicrobial peptides from their interactions with model phospholipid membranes? Peptides 24 (2003) 1693–1703.
[6] A. Giuliani, G. Pirri, S. Nicoletto, Antimicrobial peptides: an overview of a promising class of therapeutics, Cent. Eur. J. Biol. 2 (2007) 1–33.
[7] Y.J. Gordon, E.G. Romanowski, A.M. McDermott, A review of antimicrobial peptides and their therapeutic potential as anti-infective drugs, Curr. Eye Res. 30 (2005) 505–515.
[8] A.M. McDermott, Cationic antimicrobial peptides. A future therapeutic option? Arch. Soc. Esp. Oftalmol. 82 (2007) 467–470.
[9] L. Zhang, T.J. Falla, Cationic antimicrobial peptides—an update, Expert Opin. Invest. Drugs 13 (2004) 97–106.
[10] D. Takahashi, S.K. Shukla, O. Prakash, G. Zhang, Structural determinants of host defense peptides for antimicrobial activity and target cell selectivity, Biochimie 92 (2010) 1236–1241.
[11] L.M. Yin, M.A. Edwards, J. Li, C.M. Yip, C.M. Deber, Roles of hydrophobicity and charge distribution of cationic antimicrobial peptides in peptide–membrane interactions, J. Biol. Chem. 287 (2012) 7738–7745.
[12] M.M. Domingues, R.G. Inacio, J.M. Raimundo, M. Martins, M.A. Castanho, N.C. Santos, Biophysical characterization of polymyxin B interaction with LPS aggregates and membrane model systems, Biopolymers 98 (2012) 338–344.
[13] M.N. Melo, M.A. Castanho, The mechanism of action of antimicrobial peptides: lipid vesicles vs. bacteria, Front. Immunol. 3 (2012) 236.
[14] W.C. Wimley, K. Hristova, Antimicrobial peptides: successes, challenges and unanswered questions, J. Membr. Biol. 239 (2011) 27–34.
[15] R. Gautier, D. Douguet, B. Antonny, G. Drin, HELIQUEST: a web server to screen sequences with specific alpha-helical properties, Bioinformatics 24 (2008) 2101–2102.
[16] E. Lacroix, A.R. Viguera, L. Serrano, Elucidating the folding problem of alpha-helices: local motifs, long-range electrostatics, ionic-strength dependence and prediction of NMR parameters, J. Mol. Biol. 284 (1998) 173–191.
[17] Performance Standards for Antimicrobial Susceptibility Testing, Twenty Second Informational Supplement. vol. 32 N° 3, 2012.
[18] E. Strandberg, D. Tiltak, M. Ieronimo, N. Kanithasen, P. Wadhwani, A.S. Ulrich, Influence of C-terminal amidation on the antimicrobial and hemolytic activities of cationic α-helical peptides, Pure Appl. Chem. 79 (4) (2007) 717–728.
[19] S.-H. Lee, S.-J. Kim, Y.-S. Lee, M.-D. Song, I.-H. Kim, H.-S. Won, De novo generation of short antimicrobial peptides with simple amino acid composition, Regul. Pept. 166 (2011) 36–41.
[20] M. Kubista, R. Sjoback, S. Eriksson, B. Albinsson, Experimental correction for the inner-filter effect in fluorescence spectra, Analyst 119 (1994) 417–419.
[21] A.S. Ladokhin, S. Jayasinghe, S.H. White, How to measure and analyze tryptophan fluorescence in membranes properly, and why bother? Anal. Biochem. 285 (2000) 235–245.
[22] L.D. Mayer, M.J. Hope, P.R. Cullis, Vesicles of variable sizes produced by a rapid extrusion procedure, Biochim. Biophys. Acta 858 (1986) 161–168.
[23] F. Szoka, F. Olson, T. Heath, W. Vail, E. Mayhew, D. Papahadjopoulos, Preparation of unilamellar liposomes of intermediate size (0. 1–0.2 mumol) by a combination of reverse phase evaporation and extrusion through polycarbonate membranes, Biochim. Biophys. Acta 601 (1980) 559–571.
[24] F. Nicol, S. Nir, F.C. Szoka, Effect of phospholipid composition on an amphipathic peptide–mediated pore formation in bilayer vesicles, Biophys. J. 78 (2000) 818–829.
[25] N.C. Santos, M. Prieto, M.A. Castanho, Quantifying molecular partition into model systems of biomembranes: an emphasis on optical spectroscopic methods, Biochim. Biophys. Acta 1612 (2003) 123–135.
[26] S.W. Chiu, S. Subramaniam, E. Jakobsson, Simulation study of a gramicidin/lipid bilayer system in excess water and lipid. II. Rates and mechanisms of water transport, Biophys. J. 76 (1999) 1939–1950.
[27] H.G. Franquelim, L.M. Loura, N.C. Santos, M.A. Castanho, Sifuvirtide screens rigid membrane surfaces. establishment of a correlation between efficacy and membrane domain selectivity among HIV fusion inhibitor peptides, J. Am. Chem. Soc. 130 (2008) 6215–6223.
[28] N.C. Santos, M. Castanho, Fluorescence spectroscopy methodologies on the study of proteins and peptides. On the 150th anniversary of protein fluorescence, Trends Appl. Spectrosc. 4 (2002) 113–125.
[29] M. Yamazaki, M. Miyazu, T. Asano, A. Yuba, N. Kume, Direct evidence of induction of interdigitated gel structure in large unilamellar vesicles of dipalmitoylphosphatidylcholine by ethanol: studies by excimer method and high-resolution electron cryomicroscopy, Biophys. J. 66 (1994) 729–733.
[30] N.C. Santos, M. Prieto, M.A.R.B. Castanho, Interaction of the major epitope region of HIV protein gp41 with membrane model systems. A fluorescence spectroscopy study, Biochemistry 37 (1998) 8674–8682.
[31] J.F. Nagle, M.C. Wiener, Structure of fully hydrated bilayer dispersions, Biochim. Biophys. Acta 942 (1988) 1–10.
[32] P.M. Matos, M.A.R.B. Castanho, N.C. Santos, HIV-1 fusion inhibitor peptides enfuvirtide and T-1249 interact with erythrocyte and lymphocyte membranes, PLoS One 5 (2010) e9830.
[33] P.M. Matos, T. Freitas, M.A.R.B. Castanho, N.C. Santos, The role of blood cell membrane lipids on the mode of action of HIV-1 fusion inhibitor sifuvirtide, Biochem. Biophys. Res. Commun. 403 (2010) 270–274.
[34] E. Gross, R.S. Bedlack Jr., L.M. Loew, Dual-wavelength ratiometric fluorescence measurement of the membrane dipole potential, Biophys. J. 67 (1994) 208–216.
[35] R.J. Clarke, D.J. Kane, Optical detection of membrane dipole potential: avoidance of fluidity and dye-induced effects, Biochim. Biophys. Acta: Protein Struct. Mol. Enzymol. 1323 (1997) 223–239.
[36] J. Cladera, P. O'Shea, Intramembrane molecular dipoles affect the membrane insertion and folding of a model amphiphilic peptide, Biophys. J. 74 (1998) 2434–2442.
[37] D. Faccone, O. Veliz, A. Corso, M. Noguera, M. Martinez, C. Payes, L. Semorile, P.C. Maffia, Antimicrobial activity of de novo designed cationic peptides against multi-resistant clinical isolates, Eur. J. Med. Chem. 71 (2014) 31–35.
[38] M.M. Domingues, S.C. Lopes, N.C. Santos, A. Quintas, M.A. Castanho, Fold-unfold transitions in the selectivity and mechanism of action of the N-terminal fragment of the bactericidal/permeability-increasing protein (rBPI(21)), Biophys. J. 96 (2009) 987–996.
[39] M. Castanho, M. Prieto, Filipin fluorescence quenching by spin-labeled probes: studies in aqueous solution and in a membrane model system, Biophys. J. 69 (1995) 155–168.
[40] M.A. Castanho, M.J. Prieto, Fluorescence quenching data interpretation in biological systems. The use of microscopic models for data analysis and interpretation of complex systems, Biochim. Biophys. Acta 1373 (1998) 1–16.
[41] M.X. Fernandes, J. Garcia de la Torre, M.A.R.B. Castanho, Joint determination by Brownian dynamics and fluorescence quenching of the in-depth location profile of biomolecules in membranes, Anal. Biochem. 307 (2002) 1–12.
[42] P.M. Matos, M.A. Castanho, N.C. Santos, HIV-1 fusion inhibitor peptides enfuvirtide and T-1249 interact with erythrocyte and lymphocyte membranes, PLoS One 5 (2010) e9830.
[43] F. Vigant, A. Hollmann, J. Lee, N.C. Santos, A.N. Freiberg, M.E. Jung, B. Lee, The rigid amphipathic fusion inhibitor dUY11 ats through photosensitization of viruses, J. Virol. (2013).
[44] Y. Chen, M.T. Guarnieri, A.I. Vasil, M.L. Vasil, C.T. Mant, R.S. Hodges, Role of peptide hydrophobicity in the mechanism of action of alpha-helical antimicrobial peptides, Antimicrob. Agents Chemother. 51 (2007) 1398–1406.
[45] M. Mihajlovic, T. Lazaridis, Charge distribution and imperfect amphipathicity affect pore formation by antimicrobial peptides, Biochim. Biophys. Acta 1818 (2012) 1274–1283.
[46] S. Troeira Henriques, M. Nuno Melo, M.A.R.B. Castanho, How to address CPP and AMP translocation? Methods to detect and quantify peptide internalization in vitro and in vivo, Mol. Membr. Biol. 24 (2007) 173–184.
[47] M.A.R.B. Castanho, M.X. Fernandes, Lipid membrane-induced optimization for ligand–receptor docking: recent tools and insights for the membrane catalysis model, Eur. Biophys. J. 35 (2006) 92–103.
[48] A.M. Bouchet, N.B. Iannucci, M.B. Pastrian, O. Cascone, N.C. Santos, E.A. Disalvo, A. Hollmann, Biological activity of antibacterial peptides matches synergism between electrostatic and non electrostatic forces, Colloids Surf. B: Biointerfaces 114 (2014) 363–371.
[49] C. Subbalakshmi, E. Bikshapathy, N. Sitaram, R. Nagaraj, Antibacterial and hemolytic activities of single tryptophan analogs of indolicidin, Biochem. Biophys. Res. Commun. 274 (2000) 714–716.
[50] L. Silvestro, P.H. Axelsen, Membrane-induced folding of cecropin A, Biophys. J. 79 (2016) 1465–1477.
[51] K.A. Henzler Wildman, D.-K. Lee, A. Ramamoorthy, Mechanism of lipid bilayer disruption by the human antimicrobial peptide, LL-37, Biochemistry 42 (2003) 6545–6558.
[52] B. Bechinger, The structure, dynamics and orientation of antimicrobial peptides in membranes by multidimensional solid-state NMR spectroscopy, Biochim. Biophys. Acta (BBA) —Biomembr. 1462 (1999) 157–183.
[53] A. Mecke, D.-K. Lee, A. Ramamoorthy, B.G. Orr, M.M. Banaszak Holl, Membrane thinning due to antimicrobial peptide binding: an atomic force microscopy study of MSI-78 in lipid bilayers, Biophys. J. 89 (2016) 4043–4050.
[54] W.T. Heller, A.J. Waring, R.I. Lehrer, T.A. Harroun, T.M. Weiss, L. Yang, H.W. Huang, Membrane thinning effect of the β-sheet antimicrobial protegrin, Biochemistry 39 (2000) 139–145.